CHAPTER 5

ANALYSIS OF HARMONIC PLANE WAVE PROPAGATION PREDICTED BY MODIFIED GREEN-LINDSAY THERMOELASTICITY THEORY

5.1 Introduction[1]

Study of plane wave propagation through a medium is a topic of immense interest amongst the researchers. Lessen (1957), Deresiewicz (1957), Chadwick and Sneddon (1958) are among the first researchers who discussed the propagation of waves in a thermoelastic solid under classical thermoelasticity theory. Puri (1972; 1973) studied the plane waves in classical thermoelasticity (Biot (1956)), magneto-thermoelasticity and Lord-Shulman thermoelasticity theory. Agarwal (1979) looked upon the propagation and stability of harmonically time-dependent thermoelastic plane waves under GL theory. Roychoudhuri and Mukhopadhyay (2000) analyzed plane waves in generalized thermo-viscoelasticity with effects of rotation and relaxation times. Further, Puri and Jordan (2004; 2006) investigated propagation of plane harmonic waves in medium for GN-III and two-temperature thermoelasticity theory. Sharma (2007) focused on wave propagation in anisotropic medium for generalized thermoelasticity theory. Prasad et al. (2010) examined plane waves in isotropic medium for dual-phase-lag thermoelasticity

[1]The content of this chapter is published in *Waves in Random and Complex Media*, 2020.

theory. Plane wave propagation in anisotropic medium under the theory of three-phase-lag model and dual-phase-lag model was studied by Kumar and Chawla (2011). Suh and Burger (1998) differently studied the wave nature in LS and GL theory by analyzing the effects of relaxation times and thermomechanical coupling. Tiwari and Mukhopadhyay (2017) highlighted the nature of electromagneto-thermoelastic plane waves under GN-II thermoelasticity theory. Kumari et al. (2019) emphasized on wave propagation under thermoelasticity theory with a single delay term given by Quintanilla (2011).

The present thesis is aimed at investigating various problems of thermo-mechanical interactions under some recently developed thermoelasticity theories. In Chapter 4, the modified Green-Lindsay (MGL) thermoelasticity theory has been considered for investigation and Galerkin-type representation of solution for the system of equations of motion followed by general solution of homogeneous system of equations for steady oscillations has been presented. Now, to further elaborate the behavior of thermoelastic interactions under this generalized thermoelastic model, analysis of thermoelastic waves is worth pursuing. Therefore, the present chapter is devoted to highlight the specific features of the MGL theory by analyzing plane harmonic wave propagation in an isotropic homogeneous thermoelastic medium. The behavior of various qualitative characterizations of longitudinal waves is investigated in a detailed way. In order to show the differences in predictions of the present model as compared to other existing models, the problem is formulated in the contexts of MGL model along with the classical model and GL model. In order to proceed in this direction, firstly in Section 5.2, the governing equations are expressed in a unified way by considering the constitutive relations and basic equations for all three models including MGL thermoelasticity theory. Using the non-dimensional versions of the field equations, derivation of unified dispersion relation is carried out for longitudinal plane waves, in Section 5.3. Two different modes of longitudinal wave are identified. Further, Section 5.4 derives the expressions for wave number and attenuation coefficient of both the waves. Next, in Section 5.5,

computational work is carried out for a particular material and numerical results are presented by using graph profiles for different wave characteristics such as phase velocity, specific loss, and penetration depth. Comparison among three thermoelastic models and effects of dimensionless relaxation parameters involved in MGL model are discussed in a detailed way. Lastly, the important findings of the present work highlighting some specific predictions of MGL model are presented in Section 5.6.

5.2 Basic Governing Equations

Consider a fixed rectangular Cartesian co-ordinate system Ox_i, $i = 1, 2, 3$, for an unbounded isotropic homogeneous thermoelastic medium. The qualitative nature of plane wave under strain and temperature rate-dependent theory is aimed to be investigated. Hence, in order to obtain effects of strain-rate and temperature-rate terms on plane wave propagation inside the medium, a system of unified basic equations and constitutive relations in the context of linear theories of classical (Biot (1956)), GL (1972), and MGL (2018) thermoelastic models in the absence of body forces and heat sources is considered as follows:

Equation of motion:

$$\sigma_{ij,j} = \rho\, \ddot{u}_i. \tag{5.2.1}$$

Fourier's heat conduction law:

$$q_i = -K\, \theta_{,i}. \tag{5.2.2}$$

Energy equation:

$$-\, q_{i,i} = \rho\, T_0 \dot{S}. \tag{5.2.3}$$

Entropy equation:

$$T_0\,\rho\,S = \rho\,c_E\left(\theta + \tau_0\,\dot{\theta}\right) + \beta\,T_0\left(e_{kk} + m\,\tau_0\,\dot{e}_{kk}\right). \tag{5.2.4}$$

Stress-strain-temperature relation:

$$\sigma_{ij} = \lambda\left(e_{kk} + n\,\tau_1\,\dot{e}_{kk}\right)\delta_{ij} + 2\mu\left(e_{ij} + n\,\tau_1\,\dot{e}_{ij}\right) - \beta\left(\theta + \tau_1\dot{\theta}\right)\delta_{ij}. \tag{5.2.5}$$

Strain-displacement relation:

$$e_{ij} = \frac{1}{2}\left(u_{i,j} + u_{j,i}\right). \tag{5.2.6}$$

In the above equations, τ_0, and τ_1 represent relaxation times with $\tau_1 \geq \tau_0 > 0$, whereas n and m are used as constant parameters.

With the help of the above basic equations, the unified governing equations in terms of displacement and thermal fields are obtained in the following way:

Firstly, heat conduction equation can be obtained by combining Eqs. (5.2.2-5.2.4) and Eq. (5.2.6) as

$$K\,\theta_{,ii} = \rho\,c_E\left(\dot{\theta} + \tau_0\,\ddot{\theta}\right) + \beta\,T_0\left(\dot{u}_{i,i} + m\,\tau_0\,\ddot{u}_{i,i}\right). \tag{5.2.7}$$

Then, Eq. (5.2.1), Eq. (5.2.5) and Eq. (5.2.6) together yield the second field equation, i.e., displacement equation of motion, which can be expressed as

$$\rho\,\ddot{u}_i = (\lambda + \mu)\left(u_{k,ki} + n\,\tau_1\,\dot{u}_{k,ki}\right) + \mu\left(u_{i,kk} + n\,\tau_1\,\dot{u}_{i,kk}\right) - \beta\left(\theta_{,i} + \tau_1\dot{\theta}_{,i}\right). \tag{5.2.8}$$

The corresponding set of equations representing to the generalized linear thermoelasticity theories in the context of three different models can be extracted from above set of equations (5.2.1-5.2.8) for different considerations on relaxation times and the parameters, n and m in the following way:

- Classical model (Biot): $\tau_0 = \tau_1 = 0$.

- GL model: $\tau_0 \neq 0,\ \tau_1 \neq 0,$ and $n = m = 0.$

- MGL model: $\tau_0 \neq 0,\ \tau_1 \neq 0,$ and $n = m = 1.$

In order to proceed further and make analysis on plane waves convenient, the following non-dimensional transformations of variables are used:

$$x_i' = \frac{x_i}{c_0\, t_0},\ t' = \frac{t}{t_0},\ u_i' = \frac{u_i}{c_0\, t_0},\ \theta' = \frac{\theta}{T_0},\ \tau_p' = \frac{\tau_p}{t_0}\,(p = 0, 1),$$

where, $c_0^2 = \frac{\lambda+2\mu}{\rho}$ and $t_0(> 0)$ is the characteristic response time for the medium. Therefore, Eqs. (5.2.7-5.2.8) take the following forms in terms of non-dimensional field variables and parameters:

$$K_1\, \theta_{,ii} = \left(\dot{\theta} + \tau_0\, \ddot{\theta}\right) + \beta_0\, (\dot{u}_{i,i} + m\, \tau_0\, \ddot{u}_{i,i}), \tag{5.2.9}$$

$$\ddot{u}_i \ = a_1(u_{k,ki} + n\, \tau_1\, \dot{u}_{k,ki}) + a_2\, (u_{i,kk} + n\, \tau_1\, \dot{u}_{i,kk}) - \beta_1 \left(\theta_{,i} + \tau_1 \dot{\theta}_{,i}\right), \tag{5.2.10}$$

where, the primes are dropped for simplicity and the following dimensionless notations are introduced:

$$K_1 = \frac{K}{c_0^2\, t_0\, \rho\, c_E},\ \beta_0 = \frac{\beta}{\rho\, c_E},\ \beta_1 = \frac{\beta\, T_0}{\rho\, c_0^2},\ a_1 = \frac{\lambda + \mu}{\rho\, c_0^2},\ \text{and}\ a_2 = \frac{\mu}{\rho\, c_0^2}.$$

5.3 Harmonic Plane Wave

By examining the above field equations, one can easily observe that the transverse wave is not modified by, nor contribute to, the temperature field of the medium. However, the longitudinal wave is coupled with the elastic and thermal field, and therefore major attention is paid on the propagation of longitudinal wave to examine the propagation of harmonic plane waves in the present context. Hence, the results are to be analyzed using longitudinal plane wave solutions of the problem in the following forms:

$$u_j = \mathfrak{A} d_j \exp[\mathrm{i}(\omega t - \gamma\, n_k\, x_k)], \tag{5.3.1}$$

$$\theta = \mathfrak{B}\, \exp[\mathrm{i}(\omega t - \gamma\, n_k\, x_k)], \tag{5.3.2}$$

where, $\mathfrak{A}$ and $\mathfrak{B}$ represent amplitudes of waves. γ denotes complex wave number. $\omega\,(>0)$ represents the dimensionless angular frequency and $\mathrm{i} = \sqrt{-1}$. d_j and n_j denote components of unit vector in the direction of the displacement and normal to the wavefront, respectively, whereas x_k is the component of position vector. Obviously, for physically realistic nature of wave, $\mathrm{Re}[\gamma] > 0$ and $\mathrm{Im}[\gamma] \leq 0$ must hold. Further, in view of longitudinal plane waves, $d_j n_j = 1$. Phase velocity of wave is therefore given by $\frac{\omega}{\mathrm{Re}(\gamma)}$, that adapt to the longitudinal waves for which frequency and wavelength are given by $\frac{\omega}{2\pi}$ and $\frac{2\pi}{\mathrm{Re}(\gamma)}$, respectively.

5.3.1 Derivation of Dispersion Relation

Since, the harmonic plane waves (Eqs. (5.3.1-5.3.2)) are assumed to be the solution of system of Eqs. (5.2.9-5.2.10), therefore, after substituting Eqs. (5.3.1-5.3.2) into Eqs. (5.2.9-5.2.10), the following equations are acquired:

$$[\beta_0(1 + m\,\tau_0\,\mathrm{i}\,\omega)\gamma\,\omega]\,\mathfrak{A} + \left[(\mathrm{i} - \tau_0\omega)\omega + K_1\gamma^2\right]\mathfrak{B} = 0, \tag{5.3.3}$$

and

$$\left[a_1\gamma^2 n_j(1 + n\,\tau_1\,\omega\,\mathrm{i}) + a_2\gamma^2 d_j(1 + n\,\tau_1\,\omega\,\mathrm{i}) - \omega^2 d_j\right]\mathfrak{A} + [\beta_1\gamma\, n_j(\tau_1\,\omega - \mathrm{i})]\,\mathfrak{B} = 0. \tag{5.3.4}$$

Next, multiplying Eq. (5.3.4) with d_j and using $d_j n_j = 1$ along with $d_j d_j = 1$ gives

$$\left[\gamma^2(1 + n\,\tau_1\,\omega\,\mathrm{i}) - \omega^2\right]\mathfrak{A} + [\beta_1\gamma\,(\tau_1\,\omega - \mathrm{i})]\,\mathfrak{B} = 0, \tag{5.3.5}$$

where, $a_1 + a_2 = 1$.

Further, homogeneous system represented by Eq. (5.3.3) and Eq. (5.3.5) will have

non-trivial solution if the determinant of the coefficient matrix is zero, i.e.,

$$\det\begin{bmatrix} \beta_0(1+m\,\tau_0\,\mathrm{i}\,\omega)\gamma\,\omega & (\mathrm{i}-\tau_0\omega)\omega+K_1\gamma^2 \\ \gamma^2(1+n\,\tau_1\,\omega\,\mathrm{i})-\omega^2 & \beta_1\gamma\,(\tau_1\,\omega-\mathrm{i}) \end{bmatrix}=0,$$

which further gives the unified dispersion relation for the present three models as

$$\begin{aligned}\gamma^4K_1(1+n\,\tau_1\,\omega\,\mathrm{i})+\gamma^2\left[-\tau_0\omega^2-n\,\tau_1\omega^2-K_1\omega^2-\epsilon\tau_1\omega^2-m\,\tau_0\epsilon\omega^2\right.\\ \left.+\mathrm{i}(\omega-n\,\tau_0\,\tau_1\omega^3+\epsilon\,\omega-m\,\tau_1\,\tau_0\omega^3\,\epsilon)\right]-\mathrm{i}\omega^3+\tau_0\omega^4=0,\end{aligned}\tag{5.3.6}$$

where, $\epsilon=\beta_0\beta_1$ is the thermoelastic coupling parameter.

Clearly, the dispersion relations can be explicitly written for three different models as follows:

- For classical model ($\tau_0=\tau_1=0$)

$$\gamma^4K_1+\gamma^2\left[-K_1\omega^2+\mathrm{i}(\omega+\epsilon\,\omega)\right]-\mathrm{i}\omega^3=0.\tag{5.3.7}$$

- For GL model ($\tau_0\neq0$, $\tau_1\neq0$, and $n=m=0$)

$$\gamma^4K_1+\gamma^2\left[-\tau_0\omega^2-K_1\omega^2-\epsilon\tau_1\omega^2+\mathrm{i}(\omega+\epsilon\,\omega)\right]-\mathrm{i}\omega^3+\tau_0\omega^4=0.\tag{5.3.8}$$

- For MGL model ($\tau_0\neq0$, $\tau_1\neq0$, and $n=m=1$)

$$\begin{aligned}\gamma^4K_1(1+\tau_1\,\omega\,\mathrm{i})+\gamma^2\left[-(1+\epsilon)(\tau_0+\tau_1)\omega^2-K_1\omega^2+\mathrm{i}\,\omega(1+\epsilon)(1-\tau_0\,\tau_1\omega^2)\right]\\ -\mathrm{i}\omega^3+\tau_0\omega^4=0.\end{aligned}\tag{5.3.9}$$

Dispersion relation similar to Eq. (5.3.7) for the case of classical model (Biot (1956)) has been reported by Chadwick and Sneddon (1958) and similar to Eq. (5.3.8) has been reported by Agarwal (1979). Kumar et al. (2017) discussed the case of temperature-rate dependent model (GL model (1972)). Equation (5.3.9) therefore represents the dispersion relation in the context of MGL model. Moreover, Eqs. (5.3.7-5.3.9) clearly indicate the influence of additional temperature-rate and strain-rate terms as compared to the classical model.

5.4 Expressions for Wave Number and Attenuation Coefficient

Solving the dispersion relations given by Eqs. (5.3.7-5.3.9), one can find γ that represents the complex wave number where absolute value of imaginary part of γ (Im $[\gamma]$) represents attenuation coefficient. The main focus is to discuss the newly formulated MGL thermoelastic model, and therefore, Eq. (5.3.9) is now considered for this section.

Firstly, by multiplying the Eq. (5.3.9) with $(1-\tau_1\,\omega\,\mathrm{i})$ to make the leading coefficient real, one can find the following relation:

$$\gamma^4 K_1(1+\tau_1^2\,\omega^2)+\gamma^2\left\{-\omega^2\left[(1+\epsilon)\,\tau_0+K_1\right]-\omega^4\tau_0\tau_1^2(1+\epsilon)+\right.$$
$$\left.\mathrm{i}\left[\omega\,(1+\epsilon)+\tau_1\omega^3\left((1+\epsilon)\,\tau_1+K_1\right)\right]\right\}+\omega^4\,(\tau_0-\tau_1)-\mathrm{i}(\omega^3+\omega^5\tau_0\tau_1)=0. \qquad (5.4.1)$$

Next, setting $\gamma = Z\sqrt{\omega}$ in Eq. (5.4.1) yields

$$Z^4 K_1(1+\tau_1^2\,\omega^2)-Z^2\,(P-\mathrm{i}Q)+\omega^2\,(\tau_0-\tau_1)-\mathrm{i}(\omega+\omega^3\tau_0\tau_1)=0, \qquad (5.4.2)$$

where, $P=\omega\,[h\,\tau_0+K_1]+\omega^3\tau_0\tau_1^2 h,\ Q=h+\tau_1\omega^2(h\,\tau_1+K_1)$ and $h=1+\epsilon$.

Further, solving Eq. (5.4.2) as quadratic in Z^2 gives

$$Z^2 = \frac{P - \mathrm{i}Q \pm \sqrt{X + \mathrm{i}Y}}{2K_1(1 + \tau_1^2\,\omega^2)}, \tag{5.4.3}$$

where,

$$\begin{aligned}
X &= h^2\tau_0^2\tau_1^2\omega^6 - b_4\,\tau_1^2\omega^4 + b_2\omega^2 - h^2,\\
Y &= b_5\omega^5 - b_3\omega^3 + b_1\omega,\\
b_1 &= 2\left((1-\epsilon)\,K_1 - h^2\tau_0\right),\\
b_2 &= K_1^2 - 2\,(1-\epsilon)\,K_1\,(\tau_0 - \tau_1) + h^2\left(\tau_0^2 - 2\tau_1^2\right),\\
b_3 &= 2\tau_1\left(K_1^2 + 2h^2\tau_0\tau_1 - (1-\epsilon)\,K_1\,(\tau_0 + \tau_1)\right),\\
b_4 &= K_1^2 + 2\,(1-\epsilon)\,K_1\,(\tau_0 - \tau_1) + h^2\left(-2\tau_0^2 + \tau_1^2\right),\\
b_5 &= 2\tau_0\tau_1^3\left((1-\epsilon)\,K_1 - h^2\tau_1\right).
\end{aligned}$$

Next, by simplifying Eq. (5.4.3) further, the square roots of complex number Z can be found. For this, the important theorem from complex analysis (Ponnusamy (2005)) is used, according to which the following result is yielded:

$$\sqrt{X + \mathrm{i}Y} = \pm\left[\sqrt{\frac{X + \sqrt{X^2 + Y^2}}{2}} + \mathrm{i}\,\mathrm{sgn}(Y)\sqrt{\frac{-X + \sqrt{X^2 + Y^2}}{2}}\right],$$

where,

$$\mathbf{sgn}(Y) = \begin{cases} +1 & , Y \geq 0 \\ -1 & , Y < 0 \end{cases}.$$

Therefore, Eq. (5.4.3) can be rewritten as

$$Z^2 = \frac{1}{2K_1(1 + \tau_1^2\,\omega^2)}\left[P \pm \sqrt{\frac{X + \sqrt{X^2 + Y^2}}{2}} - \mathrm{i}\left(Q \mp \mathrm{sgn}(Y)\sqrt{\frac{-X + \sqrt{X^2 + Y^2}}{2}}\right)\right]. \tag{5.4.4}$$

Now, using $\gamma = Z\sqrt{\omega}$ and Eq. (5.4.4), out of four, two values of γ can be acquired such that $\text{Im}[\gamma] \leq 0$. The two modes of longitudinal harmonic waves can be identified by using these two roots. One of these modes, represented by γ_T refers to predominantly thermal-mode longitudinal wave, while other represented by γ_E represents the predominantly elastic-mode longitudinal wave.

5.5 Numerical Results and Discussion

In order to explicate the nature of wave propagation in the context of strain and temperature rate-dependent thermoelasticity theory (MGL), the numerical computations are carried out with the help of mathematical tool, Mathematica and the dispersion relations as obtained in the previous section are solved. The computational work is performed by considering the dispersion relations given by Eqs. (5.3.7-5.3.9) under all the models. Wave characteristics such as phase velocity, specific loss, and penetration depth are calculated for detailed analysis and their variations are observed with respect to ω under different theories for both thermal and elastic-mode waves. Firstly, by comparing the trend of wave components for three different thermoelastic models (classical, GL, and MGL), the effects of strain-rate term are highlighted. Later on, the variations in behavior of wave fields occurred due to different values of relaxation times, τ_0 and τ_1, in view of MGL model are pointed out. Chandrasekharaiah (1986b; 1998) and Hetnarski et al. (2009) reported in their review articles, the range of relaxation time parameters for metals at room temperature as 10^{-14} to 10^{-10}s. Also, according to the theory of MGL model, $\tau_1 \geq \tau_0 > 0$, various values of relaxation times are considered that satisfy this inequality and falls under the possible range for metals. Copper material is considered for the present analysis and due to Chadwick and Sneddon (1958), the data is taken as $\epsilon = 0.0168$ and $K_1 = 1$. Also, the following three conditions for dimensionless parameters are considered to mark the differences between the models:

Classical model (Biot): $\tau_0 = \tau_1 = 0$,

GL model: $\tau_0 = 0.01$, $\tau_1 = 0.02$, and $n = m = 0$,

MGL model: $\tau_0 = 0.01$, $\tau_1 = 0.02$, and $n = m = 1$.

Further, to observe the effects of relaxation times in case of MGL model, the following four cases are analyzed:

Case 1: $\tau_0 = 0.0025$, $\tau_1 = 0.01$,

Case 2: $\tau_0 = \tau_1 = 0.01$,

Case 3: $\tau_0 = 0.01$, $\tau_1 = 0.02$,

Case 4: $\tau_0 = 0.01$, $\tau_1 = 0.04$.

For subsequent results and discussions, notation with subscript 'T' denotes a quantity with respect to thermal-mode wave, whereas a subscript 'E' represents the quantity with respect to elastic-mode wave. Variations of different wave characteristics like, phase velocity, specific loss, and penetration depth are depicted in Figs. (5.5.1-5.5.12). The (a) part of the figures shows variations for lower range of frequencies, whereas the (b) part comprehends for the cases of higher values of frequency. Now, the following subsections provide the detailed analysis of present investigation.

5.5.1 Analysis on Phase Velocity

Phase velocity of waves in terms of angular frequency and wave number is defined by the following relation:

$$v_{T,E} = \frac{\omega}{\mathrm{Re}[\gamma_{T,E}]}. \tag{5.5.1}$$

For the considered data, the values of γ_T and γ_E are numerically extracted from the unified dispersion relation Eq. (5.3.6) by employing the conditions for physically realistic behavior, i.e., $\mathrm{Re}\,[\gamma] > 0$ and $\mathrm{Im}[\gamma] \leq 0$. Hence, the non-dimensional values of phase velocity for two modes of waves are obtained using these roots in Eq. (5.5.1).

Figures (5.5.1-5.5.2) (a,b) show the behavior of non-dimensional phase velocity for thermal and elastic-mode waves in the context of three models. Fig. 5.5.1 (b) states

that in case of new model (MGL model), the thermal-mode wave acquires a finite phase velocity similar to that in GL model which implies that the strain-rate term does not have significant effect on the motion of thermal-mode wave. For lower frequency range, Fig. 5.5.1 (a) expresses the unsubstantial effect of temperature-rate and strain-rate terms as graphs for all three models almost coincide. However, as frequency increases, phase velocity of thermal-mode wave tends a finite value ($v_T \approx 10$) in the contexts of MGL and GL models, unlike in case of classical thermoelasticity model which predicts an infinite speed of thermal-mode wave (see Fig. 5.5.1 (b)). From numerical data, it is observed that in case of MGL model, v_T starting with zero, increases rapidly for increase in frequency value and then stabilizes slowly at a finite value around 10.0 after attaining a local maximum value at non-dimensional frequency $\omega \approx 1410$.

Hence, an agreement of predictions by MGL model and GL model is found in the behavior of phase-velocity of thermal-model wave. However, these two models disagree with the prediction by classical model in this case.

Further, from Fig. 5.5.2 (b), a significant effect of strain-rate term on v_E is noted as the phase velocity of elastic-mode wave tends to infinity as ω tends to infinity under MGL model. This is a prominent difference between the three models as phase velocity of elastic-mode wave associated with classical and GL thermoelasticity theories approaches the finite value of approximately 1. Moreover, for new thermoelasticity theory (Fig. 5.5.2 (a)), v_E exhibits local minima at $\omega \approx 2.601$ with approximate minimum value of 1.002 and then increases slowly with increase in ω. The phenomenon of elastic-mode wave tending to infinity can be compared with that of thermo-viscoelasticity theory where a similar behavior of elastic-mode wave has been observed (see Roychoudhuri and Mukhopadhyay (2000)). Therefore, the addition of strain-rate term has a significant impact on propagation of elastic-mode wave. It is worth to be mentioned here that the numerical data for GL model is in full agreement with the analytical solution given by Agarwal (1979). For the case of GL model, the expressions for phase velocities

in case of lower and higher frequencies are derived as follows:

Lower Frequencies:

$$V_E \approx \sqrt{1+\epsilon}, \qquad V_T \approx \frac{(2\,K_1\omega)^{1/2}}{(1+\epsilon)^{1/2}},$$

Higher Frequencies:

$$V_E \approx \frac{2\sqrt{K_1}}{\sqrt{(K_1+\tau_0)^2+\epsilon\,K_1\tau_1}+\sqrt{(K_1-\tau_0)^2+\epsilon\,K_1\tau_1}},$$
$$V_T \approx \frac{2\sqrt{K_1}}{\sqrt{(K_1+\tau_0)^2+\epsilon\,K_1\tau_1}-\sqrt{(K_1-\tau_0)^2+\epsilon\,K_1\tau_1}}.$$

Similar expressions with different notations are derived by Agarwal(1979). Now, $\epsilon = 0.0168$, $K_1 = 1$, $\tau_0 = 0.01$, $\tau_1 = 0.02$, and $\omega = 0$ yield

$$V_E = 1.00837, \qquad V_T = 0,$$

and as $\omega \to \infty$, it is obtained that

$$V_E = 0.99983, \qquad V_T = 10.0017.$$

Hence, from Fig. 5.5.1 and Fig. 5.5.2, it is seen that the above results match perfectly with our numerical simulations in the context of phase velocity. Similarly, it has been verified for the other wave characteristics and perfect match is observed.

Next, with the help of Fig. 5.5.3 (a,b) and Fig. 5.5.4 (a,b), analysis of the impact of relaxation times, τ_0 and τ_1, on phase velocities is executed in case of MGL model. It is observed that τ_0 has significant effect on phase velocity for thermal-mode wave while τ_1 affects more on phase velocity for elastic-mode waves. Fig. 5.5.3 (b) predicts that when

τ_0 is decreased to 0.0025 (Case 1), keeping $\tau_1 = 0.01$ fixed, the finite limiting value of phase velocity for thermal-mode wave increases to 20 which is approximately double the value of v_T when $\tau_0 = 0.01$ (Case 2), whereas v_E remain unchanged (Fig 5.5.4 (b)). Further, when τ_1 is increased, keeping τ_0 fixed, negligible change in v_T is observed (Fig 5.5.3 (a,b)) while phase velocity for elastic-mode wave shows notable changes (Fig 5.5.4 (a,b)) in such case. v_E also undergoes a left shift in local minima with an increase in rate of change of values when τ_1 is increased keeping τ_0 fixed (Fig 5.5.4 (a)).

5.5.2 Analysis on Specific Loss

Specific loss ($SP_{T,E}$) in terms of wave number (Re[$\gamma_{T,E}$]) and attenuation coefficient (Im[$\gamma_{T,E}$]) is calculated by the following formula:

$$SP_{T,E} = \left(\frac{\Delta W}{W}\right)_{T,E} = 4\pi \left|\frac{\mathrm{Im}[\gamma_{T,E}]}{\mathrm{Re}[\gamma_{T,E}]}\right|. \tag{5.5.2}$$

Figure 5.5.5 (a,b) and Fig. 5.5.6 (a,b) represent the variations of specific loss for thermal-mode wave and elastic-mode wave, respectively in case of three different models. From Fig. 5.5.5 (a), it is discovered that, SP_T for new theory approaches to approximate value of 4π as ω is nearer to zero, whereas SP_T tends to 0 as ω tends to infinity. This trend is similar to the trend in case of GL theory and thereby it can be concluded that there is no effect of strain-rate term on specific loss for thermal-mode wave as observed in case of phase velocity profile. On the other hand, from Fig. 5.5.5 (a), it is noted that SP_T for classical thermoelasticity theory starts with approximate value of 4π at $\omega = 0$, attains a local minima and then again tends to 4π as ω tends to infinity. Fig. 5.5.6 (a,b) highlights the prominent differences in values of SP_E for MGL theory from that of classical and GL thermoelasticity theories. SP_E for GL and classical theory witnesses a local maxima (Fig. 5.5.6 (a)) whereas for thermoelasticity theory with additional strain-rate term, value of SP_E gradually increases from 0 to attain a limiting value approximately equal to 4π. Hence, again the major impact of

strain-rate term is observed on behaviour of elastic-mode wave in terms of specific loss.

Further, from Fig. 5.5.7 (a,b) and Fig. 5.5.8 (a,b), the variations in the values of specific loss for thermal-mode wave and elastic-mode wave, respectively are marked due to different values of relaxation times in case of MGL model. From Fig. 5.5.7 (a,b), Cases 2-4 imply that the change in value of τ_1 has negligible impact on SP_T when the value of τ_0 is fixed to 0.01. Further, Case 1 highlights the significant change in value of SP_T when value of τ_0 decreases in comparison to Case 2. Hence, decrease in values of τ_0 when τ_1 is fixed, affects the rate of decrease in values of SP_T. On the other hand, Fig. 5.5.8 (a,b) brings out a prominent effect of τ_1 on SP_E when value of τ_0 is fixed (Case 2-4). It also points out the unaffectedness of SP_E when τ_0 is changed (Case 1-2), keeping τ_1 to be fixed.

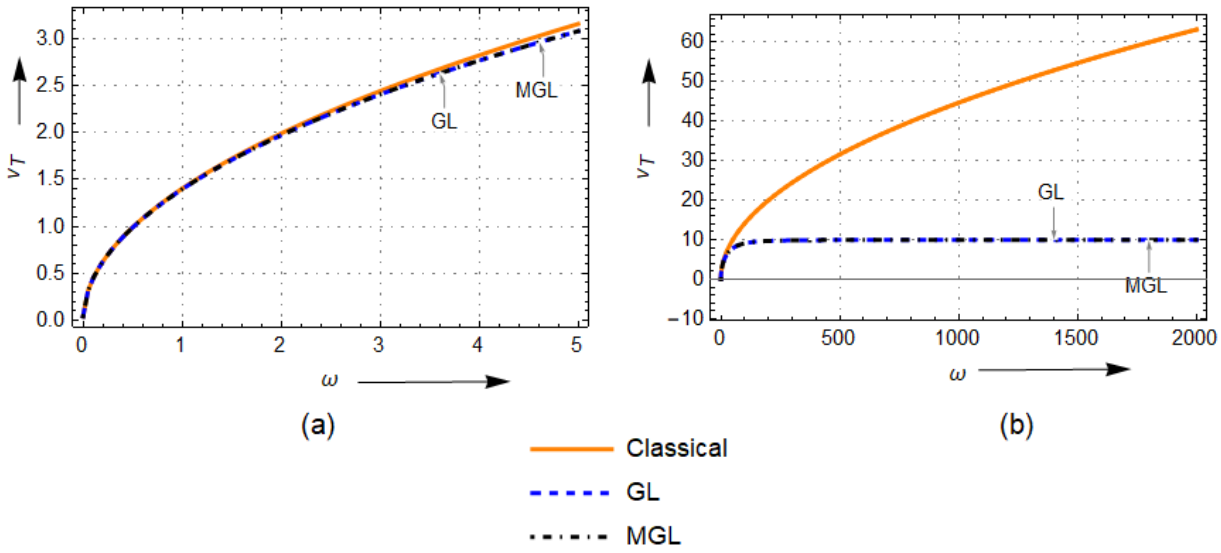

Figure 5.5.1: Variation of phase velocity for thermal-mode wave for three different models

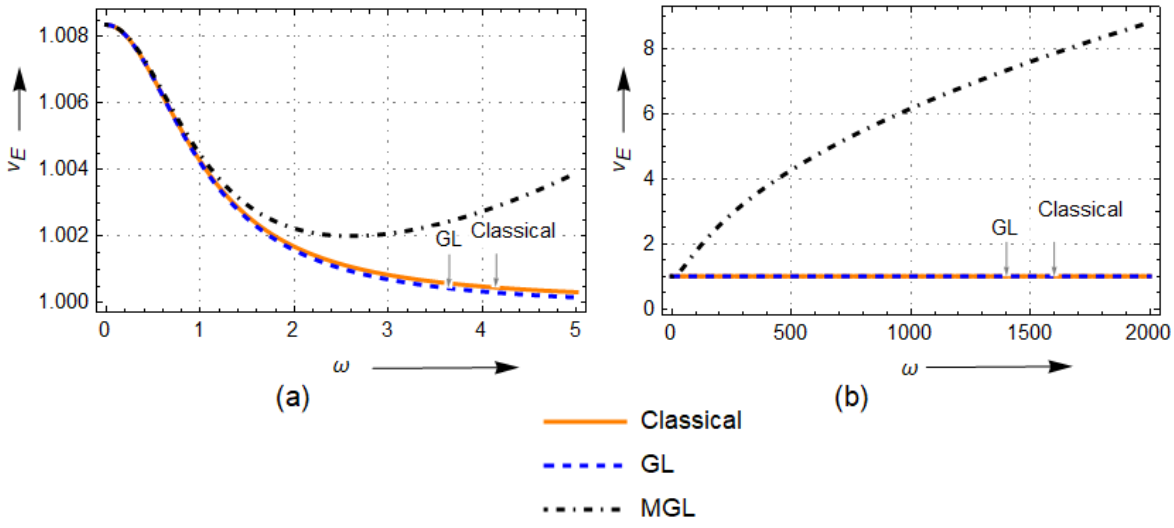

Figure 5.5.2: Variation of phase velocity for elastic-mode wave for three different models

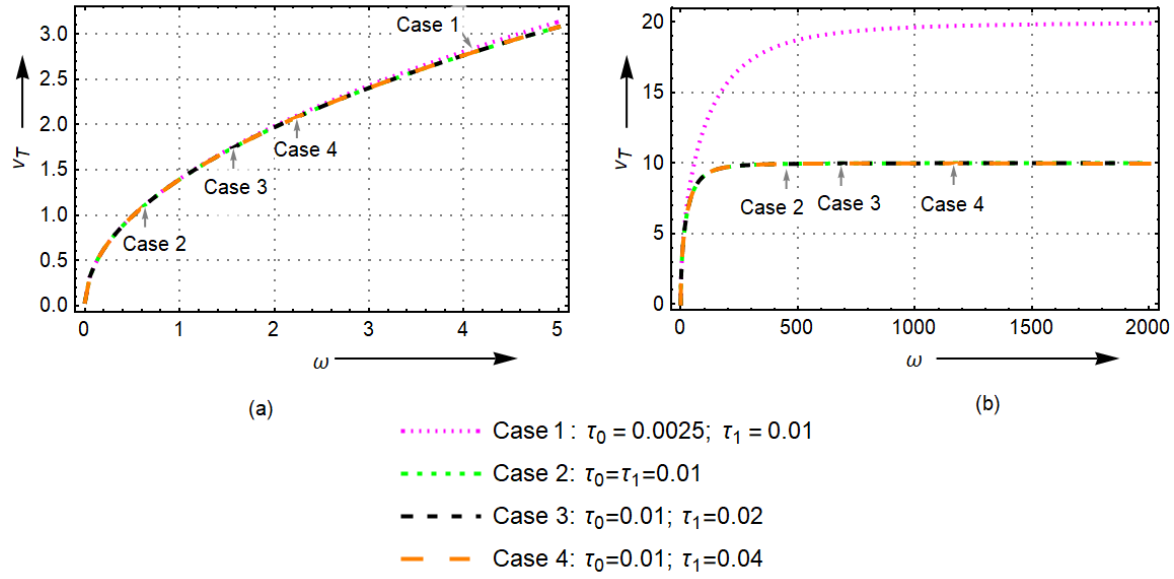

Figure 5.5.3: Variation of phase velocity for thermal-mode wave for different values of τ_0 and τ_1 for MGL model

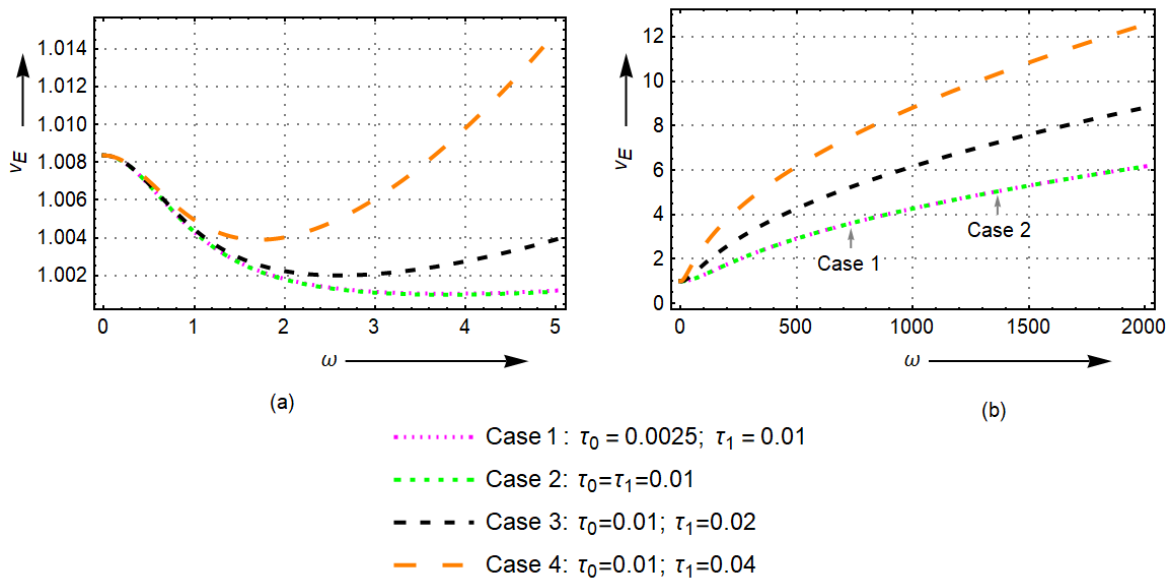

Figure 5.5.4: Variation of phase velocity for elastic-mode wave for different values of τ_0 and τ_1 for MGL model

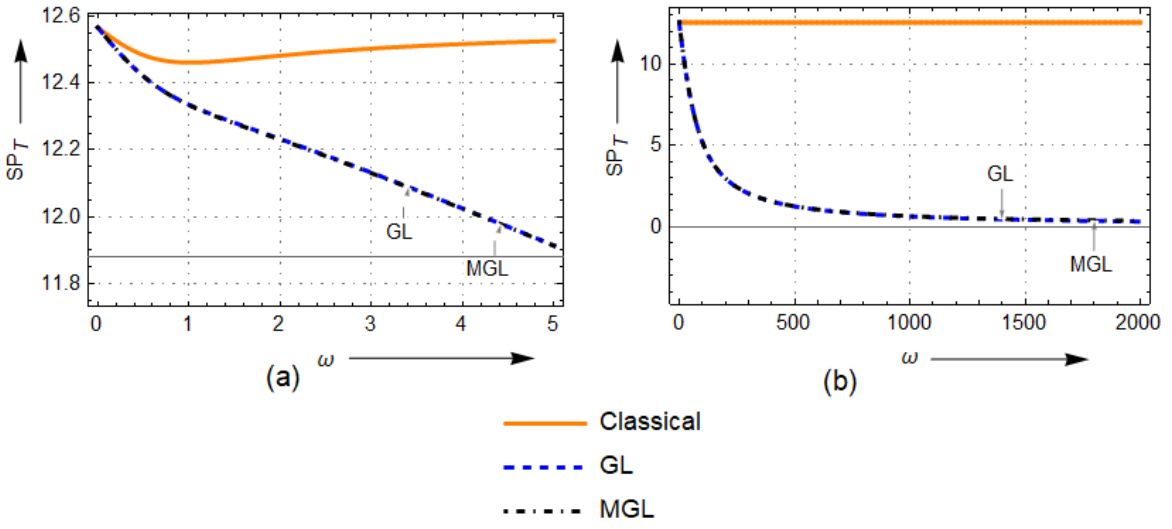

Figure 5.5.5: Variation of specific loss for thermal-mode wave for three different models

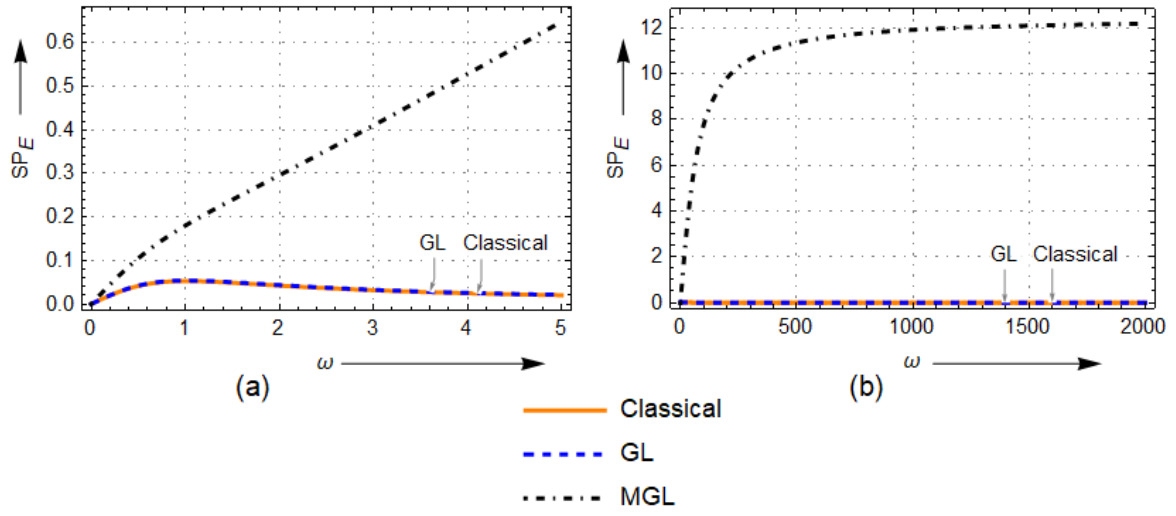

Figure 5.5.6: Variation of specific loss for elastic-mode wave for three different models

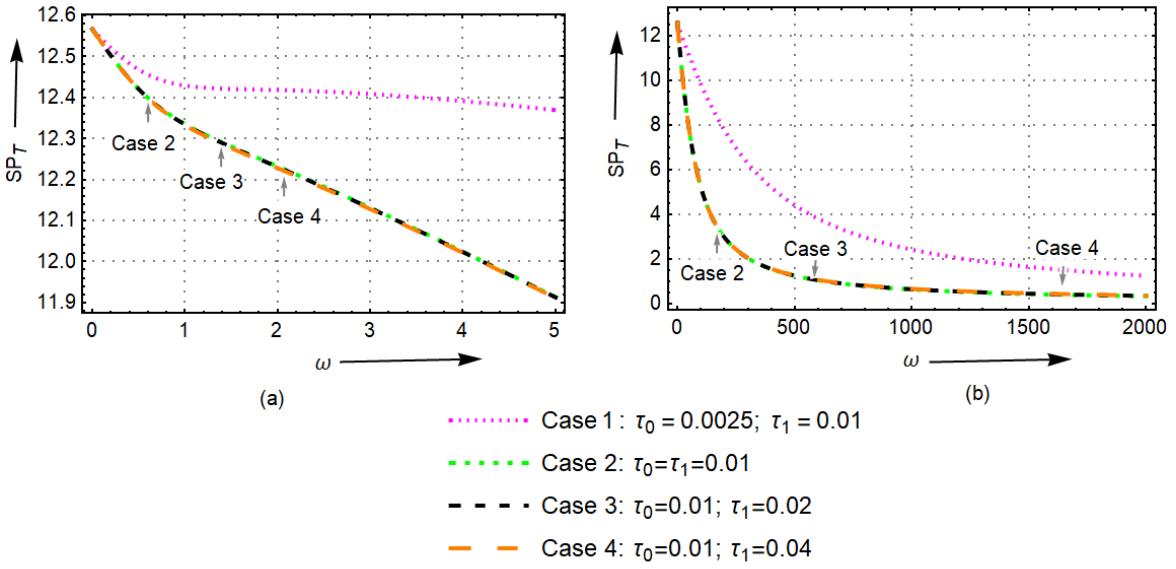

Figure 5.5.7: Variation of specific loss for thermal-mode wave for different values of τ_0 and τ_1 for MGL model

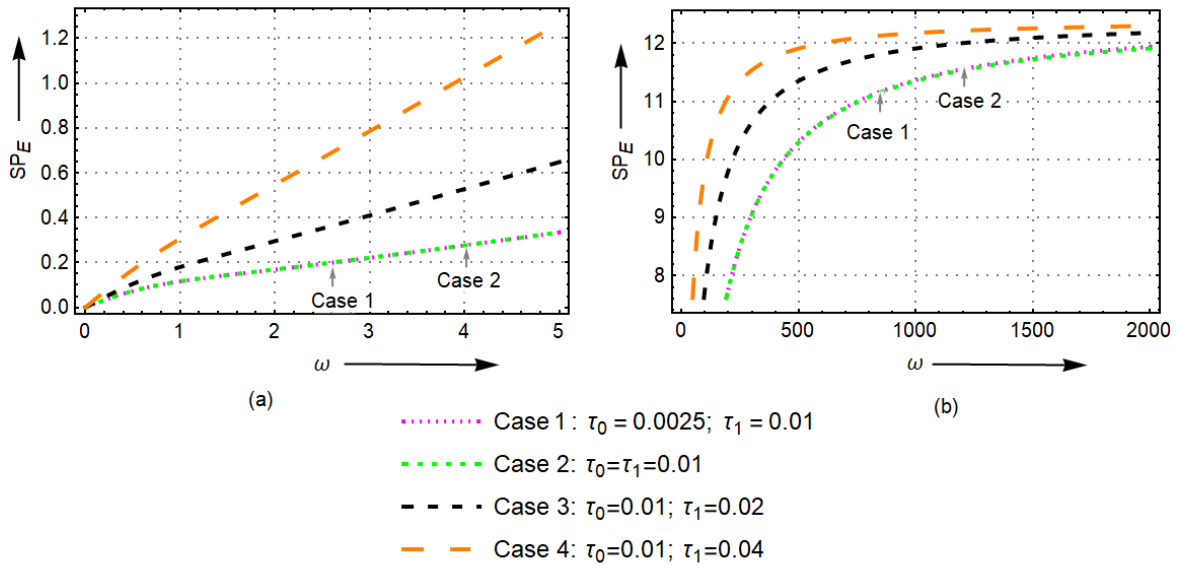

Figure 5.5.8: Variation of specific loss for elastic-mode wave for different values of τ_0 and τ_1 for MGL model

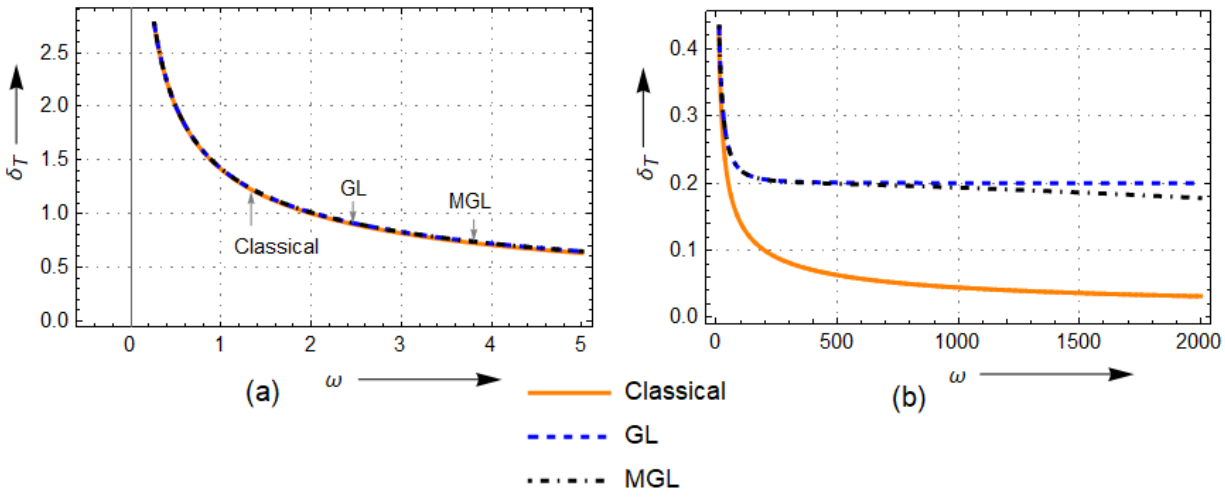

Figure 5.5.9: Variation of penetration depth for thermal-mode wave for three different models

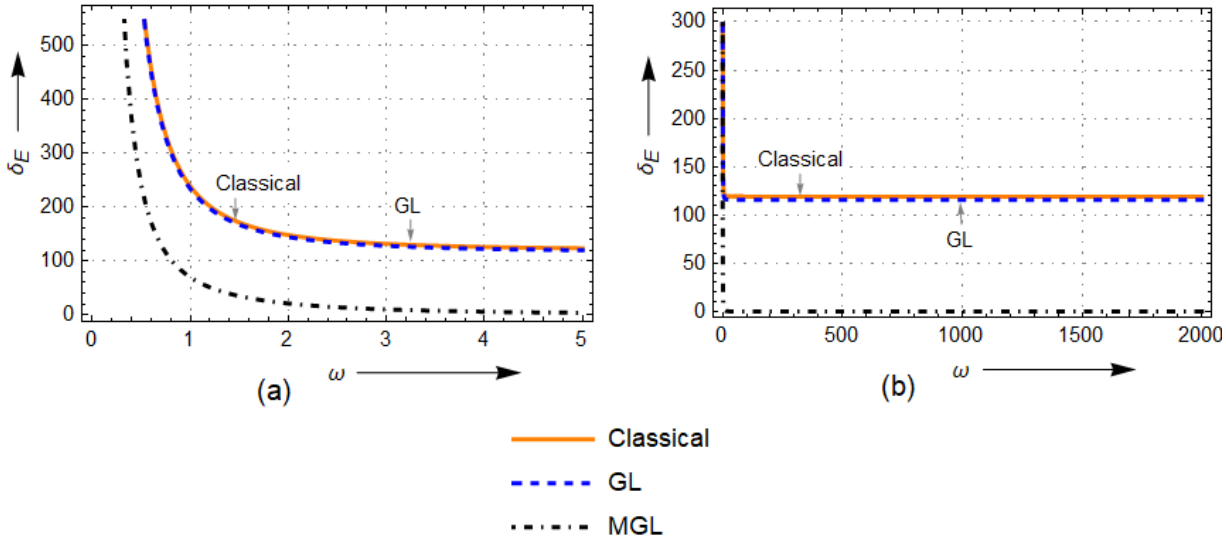

Figure 5.5.10: Variation of penetration depth for elastic-mode wave for three different models

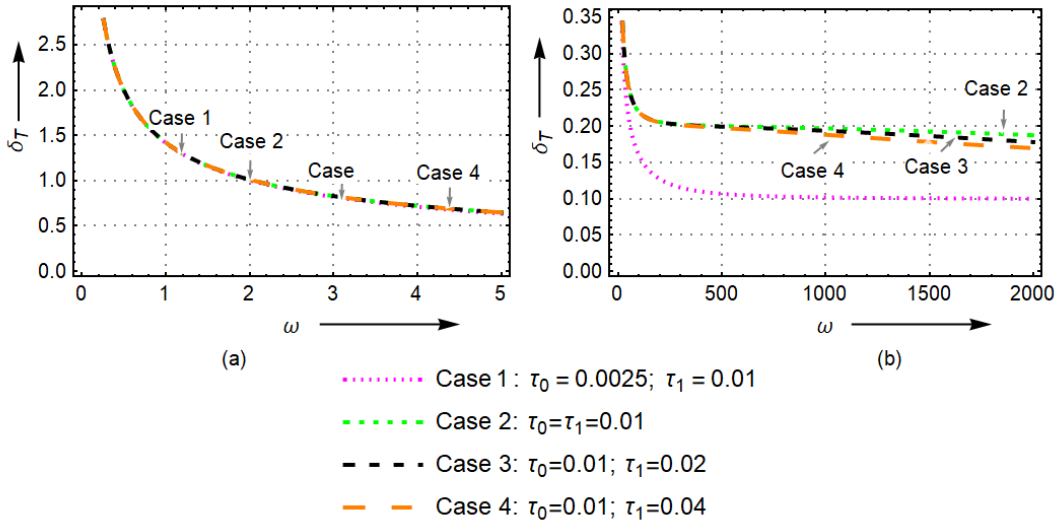

Figure 5.5.11: Variation of penetration depth for thermal-mode wave for different values of τ_0 and τ_1 for MGL model

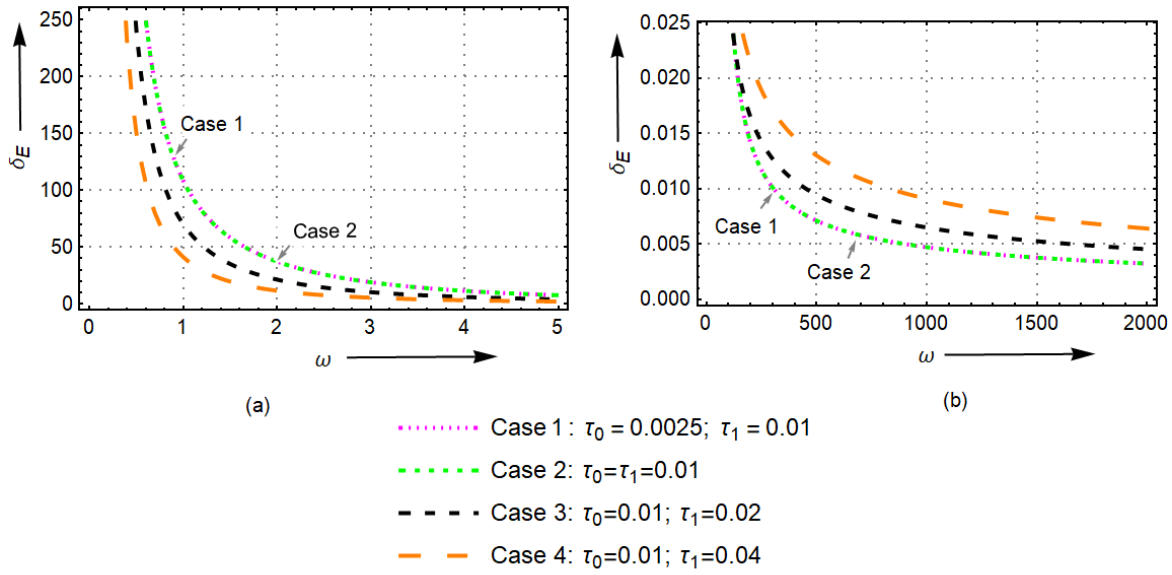

Figure 5.5.12: Variation of penetration depth for elastic wave for different values of τ_0 and τ_1 for MGL model

5.5.3 Analysis on Penetration Depth

The penetration depth ($\delta_{T,E}$) is defined by the following relation:

$$\delta_{T,E} = \left| \frac{1}{\mathrm{Im}[\gamma_{T,E}]} \right|. \tag{5.5.3}$$

Figures (5.5.9-5.5.12) (a,b) reveal the variation of penetration depth for thermal-mode and elastic-mode longitudinal waves. Fig. 5.5.9 (a,b) and Fig. 5.5.10 (a,b) show the comparison between three different models in view of penetration depth. From Fig. 5.5.9 (a), it is detected that the nature of variation of δ_T is similar for the three models for lower frequencies, i.e., influence of temperature-rate term as well as of strain-rate term is insignificant on behavior of penetration depth for lower values of frequency in case of thermal-mode wave. In general, δ_T attains infinite value for ω in neighborhood of zero and then gradually decreases to a constant value. Fig. 5.5.9 (b) adduces that the value of δ_T for classical model approaches to zero value whereas for GL and MGL model, the constant values are nearer to 0.2. The nature of δ_T for MGL theory is

similar to that of GL theory, but for higher range of frequencies, the effect of strain-rate term is observed to be prominent as the profiles of δ_T for these two models start deviating. Fig. 5.5.10 (a,b) show the same pattern of δ_E for classical and GL model. Fig. 5.5.10 (b) highlights that δ_E for classical and GL model attains constant value of 120 as $\omega \to \infty$, whereas, for MGL model, δ_E approaches to zero as $\omega \to \infty$. This pattern points out that the penetration depth for elastic-mode wave remain unaffected when temperature-rate is introduced to constitutive relations, in comparison to the classical theory, whereas further addition of strain-rate term shows a notable difference in the behavior of penetration depth of elastic-mode longitudinal wave.

Further, Fig. 5.5.11 (a,b) and Fig. 5.5.12 (a,b) illustrate the effects of relaxation times on the penetration depth for thermal-mode wave and elastic-mode wave, respectively in view of MGL theory. Fig. 5.5.11 (a) points that the change in values of relaxation times, τ_0 and τ_1, does not have any prominent effect on the δ_T for lower frequency values, whereas effect of change in values of τ_0 is observed when τ_1 is kept fixed for higher values of frequency. The limiting value of δ_T decreases when τ_0 decreases keeping τ_1 fixed. On the other hand, from 5.5.12 (a,b), it is noticed that τ_0 does not have any effect on δ_E. Further,the significant changes in values of δ_E are found when τ_1 is changed, keeping τ_0 fixed. This change in values of τ_1, keeping τ_0 fixed, affects the rate of change in values of δ_E with respect to ω.

5.6 Conclusion

In the present chapter of the thesis, propagation of harmonic plane waves in the context of modified Green-Lindsay thermoelasticity model is analyzed. To elaborate this purpose, the present problem is studied by considering three different models (classical thermoelastic model, GL model, and MGL model) and consequences of varying relaxation parameters are emphasized in the view of three important wave components such

as phase velocity, specific loss, and penetration depth. The unified governing equations for three different theories are considered and then the dispersion equation in terms of non-dimensional variables and parameters is derived in a unified way to investigate the longitudinal plane wave. Two different modes (elastic-mode and thermal-mode) of longitudinal plane wave are identified to propagate through the medium. Using solution of dispersion relation, numerical computations and graphical representations are employed to conduct the analysis of thermoelasticity theory with the effects of strain-rate and temperature-rate terms on the behavior of elastic and thermal-mode waves. The highlights of the present investigation can be outlined as follows:

- Phase velocity for thermal-mode wave in case of MGL thermoelastic model attains a finite value of 10, like the case of GL model. However, phase velocity for elastic-mode wave under MGL model tends to infinity as $\omega \to \infty$ after attaining local minima at $\omega \approx 2.601$. This behavior of phase velocity for elastic-mode wave is different from the trend observed under GL theory and classical theory predicting the fact that phase velocity for elastic-mode wave attains finite limiting values in these two cases. The similar behavior of phase velocity of elastic-mode wave predicted by MGL model is also observed in a problem related to thermo-viscoelasticity theory (Roychoudhuri and Mukhopadhyay (2000)).

- Specific loss for thermal-mode wave in the context of new thermoelasticity model starts with the value of 4π and steadily decrease to zero, which is similar to the pattern in case of GL theory. On the other hand, unlike classical and GL theory, specific loss for elastic-mode wave in case of MGL theory starts with zero and gradually attains the limiting value of 4π.

- Like the case of GL theory, penetration depth for thermal-mode wave for MGL thermoelasticity theory tends to infinity as $\omega \to 0$, whereas it approaches a finite limiting value near 0.2 as frequency increases under both the theories. Unlike

other two models, penetration depth for elastic-mode wave for MGL model starts with infinite value and gradually decreases to zero.

- Effects of relaxation parameters, τ_0 and τ_1, are observed in case of modified Green-Lindsay theory and it is worth mentioning that when τ_0 is varied keeping τ_1 fixed, the significant difference in the behavior of wave components for thermal-mode wave is obtained. On the other hand, when τ_1 is varied keeping τ_0 fixed, notable variations in the trend of wave characterizations of elastic-mode wave is observed.

- From all the graphs for three different theories, it can be concluded that the inclusion of only temperature-rate term in the constitutive relations overcomes the drawback of infinite speed behavior of thermal-mode wave predicted by classical theory. However, the addition of strain-rate term along with the temperature-rate term in the constitutive relations has a notable influence on the propagation of elastic-mode wave in comparison to that of thermal-mode wave.